Int. J. Electrochem. Sci.,8 **(2013)** 5421 -5437

International Journal of
ELECTROCHEMICAL
SCIENCE
www.electrochemsci.org

Effect of Water on the Stress Corrosion Cracking Behavior of API 5L-X52 Steel in E95 Blend

G.K. Pedraza-Basulto[1], *A.M. Arizmendi-Morquecho*[2], *J.A. Cabral Miramontes*[3], *A. Borunda-Terrazas*[1], *A. Martinez-Villafane*[1], *J.G. Chacón-Nava*[1,*]

[1] Centro de Investigación en Materiales Avanzados S.C. (CIMAV), Miguel de Cervantes # 120, Complejo. Industrial Chihuahua, Chihuahua, Chih. México, CP 31109.
[2]Centro de Investigación en Materiales Avanzados S.C. (CIMAV-Unidad Monterrey), Alianza Norte 201, Parque de Investigación e Innovación Tecnológica, Apodaca Nuevo León., México.
[3] Centro de Investigación e Innovación en Ingeniería Aeronáutica (CIIIA), Universidad Autónoma de Nuevo León (UANL), Monterey, NL. México.
[*]E-mail: jose.chacon@cimav.edu.mx

Received: 9 February 2013 / *Accepted:* 1 March 2013 / *Published:* 1 April 2013

The effect of water content (0.5%, 1%, 2%, 5%, 10% y 20 V%) in E95 blend (5 V% gasoline – 95 V% ethanol) on the stress corrosion cracking (SCC) susceptibility of X-52 carbon steel was investigated. Slow strain rate tests (SSRT) coupled with electrochemical noise measurements (ECN) were carried out using a strain rate of 1 X 10^{-6} s^{-1}. In general, scanning electron microscopy (SEM) observations on fracture surfaces showed a ductile behavior. However, secondary cracking was only observed for specimens exposed to solution containing up to 2 V% water. ECN gave indication of a likely localized corrosion process occurring at low water concentrations, whereas for water content above 2 V%, a uniform corrosion process seems more likely to occur. In addition, the material response immersed into the various solutions was investigated by using linear polarization resistance (LPR) measurements, weight loss and pH measurements. Reasons to explain the behavior found are discussed.

Keywords: Fuel-grade ethanol, X-52 steel, stress corrosion cracking, water content.

1. INTRODUCTION

Over the last few years and due to technical and environmental reasons, an important amount of efforts has been done in order to get a better understanding about the corrosion behavior of carbon steel exposed to biofuels such as bioethanol, biodiesel and biobutanol among others. The use of these biofuels represents an interesting alternative to reduce carbon emissions and replace fossil fuels. Back in 1979, the methyl-therbutyl-ether (MTBE) replaced lead as oxidant agent. Also, the use of MTBE

reduced the amount of contaminant emissions to the atmosphere. Despite of these good characteristics, MTBE is resistant to biodegradation, has high solubility in water and one consequence of this is that in the event of gasoline spillage in rain season produces soil contamination. Thus, ethanol is used as oxidant in biofuel-gasoline blends [1-3]. Ethanol also enhances the octane number and reduces the harmful effects to the atmosphere [4-5].

Due to the interest for using bioethanol as oxidant in gasoline, it is important to assess the materials performance in ethanol-gasoline blends [6]. Currently, the transport of bioethanol is by trucks, cargo-ships and railroad tanker cars. Given the high demand of bioethanol, these ways are more costly than pipeline transport, which seems a more efficient, cheap and safe way for transportation [7]. Concerns about corrosion and stress corrosion cracking (SCC) in current carbon steel pipelines in bioethanol and bioethanol-gasoline blends are major issues regarding the use of pipelines in ethanol products. It has been reported that SCC can occur within the specifications of ASTM D 4806 [8] and also within the established limits for methanol and chloride ions, these compounds might increase the steel SCC susceptibility. However, they are not essentially necessary for SCC to occur.

In non-aqueous environments such as anhydrous ammonia and methanol, the stress corrosion cracking of mild steel has been reported [9]. In the former case, it has been shown that pure anhydrous ammonia does not cause cracking, but a water content of more than 0.1% by weight can also prevent cracking in the liquid phase i.e. water acts as a corrosion inhibitor. In the latter case, slow strain rate tests (SSRT) on specimens of a steel exposed in a methanolic solution containing 10^{-4} M sulfuric acid (H_2SO_4) and 150 ppm to 10,000 ppm by weight H_2O showed that SCC occurred only when the water content was in the range from 0.1 V% to 0.5 V% [10]. Lou et. al. [11] studied the effect of water content (up to 5 V%) on the SCC of carbon steel in fuel-grade ethanol (FGE). These researchers have shown that carbon steel exposed to fuel-graded ethanol without water exhibited lower SCC susceptibility than in FGE with 1 V% water. At 5 V% water content, the carbon steel did not show signs of SCC. However, the samples showed higher tendency for localized (pitting corrosion) and general corrosion Sridhar et al. [9] and Kane et al [12] have studied the effect of water, oxygen, acetic acid, chlorides, methanol and denaturant content on the stress corrosion cracking in fuel-grade ethanol. In their work on SCC of a carbon steel exposed to a range of ethanol-gasoline blends Albistur-Goñi et. al. [5] reported that SCC was observed only in notched specimens. Lou et al. [11] reported that a transition from SCC to pitting corrosion was observed above 2.5 V% water concentration in fuel-grade ethanol.

The aim of this study is to investigate the effect of water content in E95 blend on the stress corrosion cracking of API 5L X-52 steel. In order to assess the steel mechanical and electrochemical response, slow strain rate tests (SSRT) coupled with electrochemical noise (ECN) were carried out. In addition, potential measurements, pH_e and weight loss test were carried out.

2. MATERIALS AND METHODS

2.1 Test specimens.

Specimens were taken from an API 5L-X52 pipeline steel in the as-received condition. The chemical composition obtained by chemical analysis is shown in Table 1. For the SCC tests, tensile

samples were machined according to the ASTM standard G129 [13]. All specimens were dry-ground with SiC papers up to 800 grit. Afterwards, specimens were degreased with acetone and dried under a stream of hot air.

Table 1. Chemical Composition (wt.%) of the As-Received X-52 Steel

Type	C	Mn	P	S	Si	Ni	Al	Fe
API 5L-X52	0.13	1.26	0.017	0.012	0.23	0.063	0.013	Bal.

2.2 Environments

In this work, an E95 blend (5% gasoline-95% ethanol) was used. For the fuel grade ethanol, its chemical composition was based on the ASTM standard D 4806–07, Table 2. The test solutions (prepared using analytical-grade reagents and deionized water) are shown in Table 3 and all tests were carried out at room temperature (≈ 25 C).

Table 2. Chemical composition of the baseline ethanol used in this study according to ASTM D 4806

Components	Min.	Max.	Method
Ethanol (vol%)	92.1	—	ASTM D 5501
Methanol (vol%)	—	0.55	
Solvent-washed gums (mg/100 mL)	—	5.0	ASTM D 381
Water (vol%)	—	1.0	ASTM D 6304
Denaturant (vol%)	1.96	4.76	
Inorganic chloride (mg/L)	—	32	ASTM D 512
Copper (mg/kg)	—	0.1	ASTM D 1688
Acidity as acetic acid (mg/L)	—	5.6	ASTM D 1613
pH_e	6.5	9.0	ASTM D 6423

Table 3. Composition of the various solutions used in this study.

Blend	Water V%	Ethanol V%	Acetic Acid mg/L	NaCl mg/L	Methanol V%
0.5E95	0.5	94.0	5.6	32	0.5
1E95	1	93.5	5.6	32	0.5
2E95	2	92.5	5.6	32	0.5
5E95	5	89.5	5.6	32	0.5
10E95	10	84.5	5.6	32	0.5
20E95	20	74.5	5.6	32	0.5
Inert	Glycerin				

2.3 Slow Strain Rate Test

In order to determine the SCC susceptibility of X-52 steel after exposition to the various test solutions, the experimental set-up for the slow strain rate test (SSRT) was done according to the NACE TM 0111-2011 [14] standard. A nylamid cell with poly-tetrafluoroethylene (PTFE) end caps was used. The strain rate used for this study was 1 $X10^{-6}$ s^{-1}. During the mechanical tests, the electrochemical response of the specimens was continuously monitored using the electrochemical noise (ECN) technique. A Potentiostat-Galvanostat-ZRA (ACM) was used, and the data acquisition rate was 1 point per second. Potential noise measurements were taken by using a non-aqueous Ag/AgCl/EtOH/LiCl reference electrode (RE). ECN was chosen given the fact that potential noise measurements do not need an externally applied polarization as is the case with other electrochemical techniques and thus IR potential drops and non-uniform polarization current distribution problems are effectively avoided. Also, ECN is recommended in highly resistive environments [15] such as the ones in the present work.

2.4 Linear Polarization Resistance.

In order to assess the corrosion rate of the specimens exposed to the various tests solutions, linear polarization resistance (LPR) tests were done by using an ACM Gill 1 potentiostat-galvanostat using automatic ohmic compensation. A specially adapted corrosion cell was used to avoid oxygen access into it. A three electrode arrangement was used i.e. X-52 steel as a working electrode, an Ag/AgCl/EtOH/LiCl reference electrode (which was stabilized to 100 mV vs a saturated calomel electrode (SCE) into a 100% ethanolic solution), and a platinum foil as counter electrode. Measurements were carried out by applying a small sweep from -20 to +20 mV around the corrosion potential at a scan rate of 0.16 mV/s. From the LPR data, the corrosion rates were calculated in terms of corrosion current density (Icorr) using the Stearn-Geary equation [16]. Corrosion rates in mm/y were calculated according to Faraday´s law.

2.5 Weight Loss Tests

Weight loss tests were carried out according to the ASTM G1 standard [17]. Cylindrical specimens of about 10 mm length x 10 mm diameter were immersed into the corresponding test solution (80 ml.) for 30, 60 and 90 days at room temperature. Initial and final weight measurements were taken by using a Sartorious electronic microbalance with a resolution of 10^{-5} g.

2.6 pH_e Measurements

Before and after SSRT, LPR and weight loss tests, the pH_e (defined as a measure of the acid strength of alcohol fuels containing nominally 70 volume % ethanol, or higher) values were measured [18].

2.7 Sample Observations

After exposure, the surface morphology and fracture surface of the samples were examined using a Jeol JSM 5800LV scanning electron microscope (SEM).

3. RESULTS AND DISCUSION

3.1 SSRT Tests

Fig. 1 shows the stress-strain curves obtained for type X-52 steel exposed to the various test solutions. From these results, important ductility parameters such as percent reduction in area (%RA), time to fracture or elongation to fracture can be obtained. For the evaluation of SCC susceptibility, the ratio of ductility (i.e. %RA) in the test environment vs. ductility (i.e. $\%RA_i$) in an inert environment is estimated. McIntyre et. al. [19] classified the results into five categories: Category 1.-*Immune* (i.e. show no evidence of environmental crack growth and ductility ratios equal or greater than 0.9) up to Category 5.-*Susceptible* (i.e. environmentally induced brittle fracture and extensive secondary cracking on specimen gage length occurs. Here, ductility ratios are less than 0.5.

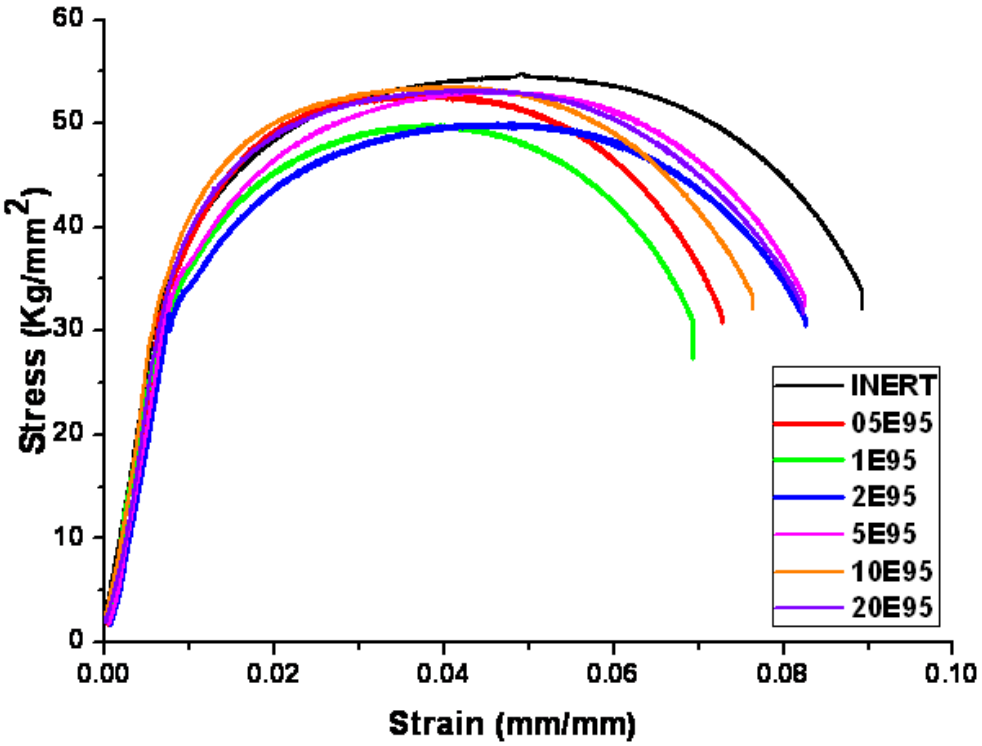

Figure 1. The stress-strain curves of the X-52 steel exposed in E95 blend with various water concentrations (V%) at room temperature.

The results of ductility parameters obtained from the SSRT tests, observations of fracture surface by SEM and open circuit potential (OCP) recorded at different stress levels i.e. yield stress

(Y.S.), maximum stress and fracture stress are shown in Table 4. It can be seen that the X-52 steel specimen exposed to solution 1E95 disclosed a value of %E ≈ 6 whereas for the inert environment %E ≈ 8. Under the present conditions, this might indicate some influence of the electrolyte acting on the specimen.

Table 4. Summary of SSRT tests obtained for X-52 steel exposed to the in E95 blend with various water concentrations (V%) at room temperature

Solution	%E	%RA	I_{RA}	SEM	OCP (mV vs Ag/AgCl/EtOH/LiCl)		
					Y.S.	Max. Stress	Fracture Stress
0.5E95	6.7321	73.4819	1.0406	Ductile morphology / Mildly Susceptible	-47	-53.3	-41
1E95	6.3437	75.9969	1.0762	Ductile morphology / Mildly Susceptible	-52.6	-054.7	-13.4
2E95	7.1573	67.2551	0.9524	Ductile morphology / Mildly Susceptible	-88.4	-105.9	-135.6
5E95	7.3203	71.91	1.0184	Ductile morphology / Immune	-91.9	-105.1	-135.6
10E95	7.5472	75.1730	1.0646	Ductile morphology / Immune	-181.5	-257.9	-277.8
20E95	8.1871	72.6416	1.0287	Ductile morphology / Immune	-540.7	-527.2	-523.8
Inert	8.0903	70.6100	1	Ductile morphology / Immune	-536.1	-533.9	-544.6

Irrespective to the solution used, the values of percent reduction of area ratio, I_{RA}, indicate no susceptibility to SCC. However, there are two factors worthy to mention: first, according to the literature [20-21] mild carbon steels in ethanolic environments might show susceptibility to SCC in a potential range from -100 mV to 400 (mV vs Ag/AgCl/EtOh/LiCl). In the present work, the potential values recorded at maximum stress for samples exposed to solutions with water content of 2 V%, 1 V % and 0.5 V% are -105.9, -54 and - 43 (mV vs Ag/AgCl/EtOH/LiCl) respectively.

Fracture Surface
0.5E95

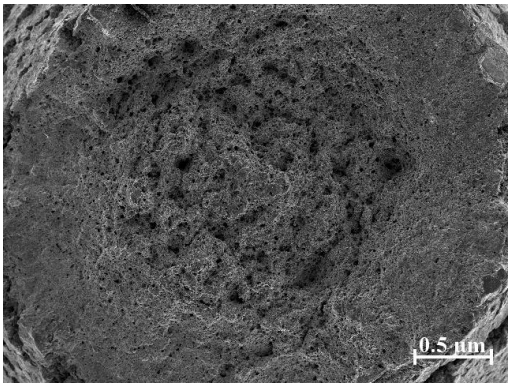

Lateral View
0.5E95

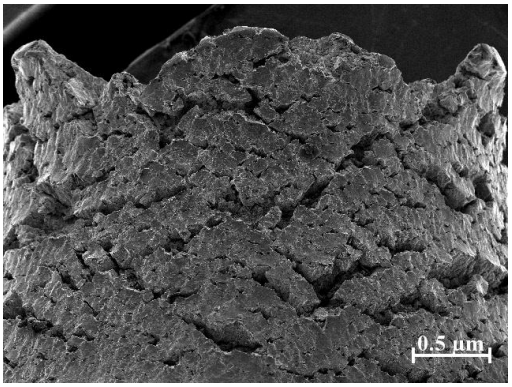

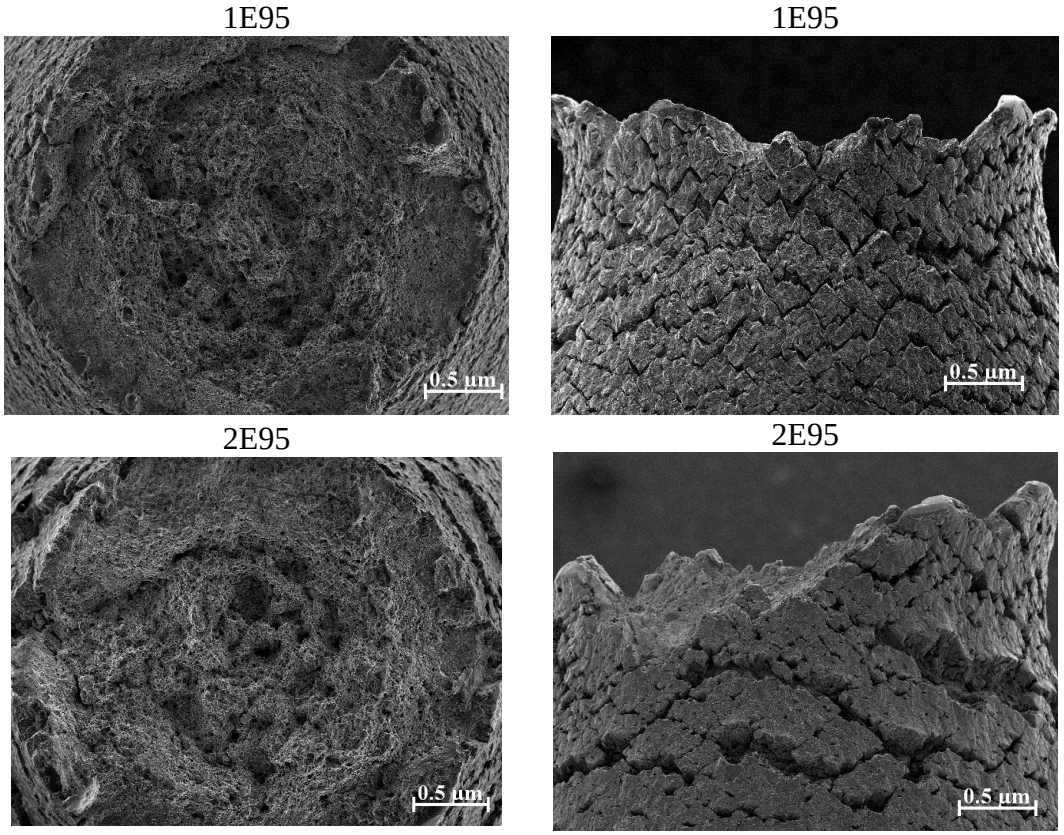

Figure 2. SEM images of a) fracture surface showing ductile failure and b) lateral view showing secondary cracks, for specimens exposed to solutions with water content of 0.5 V%, 1 V% and 2 V%.

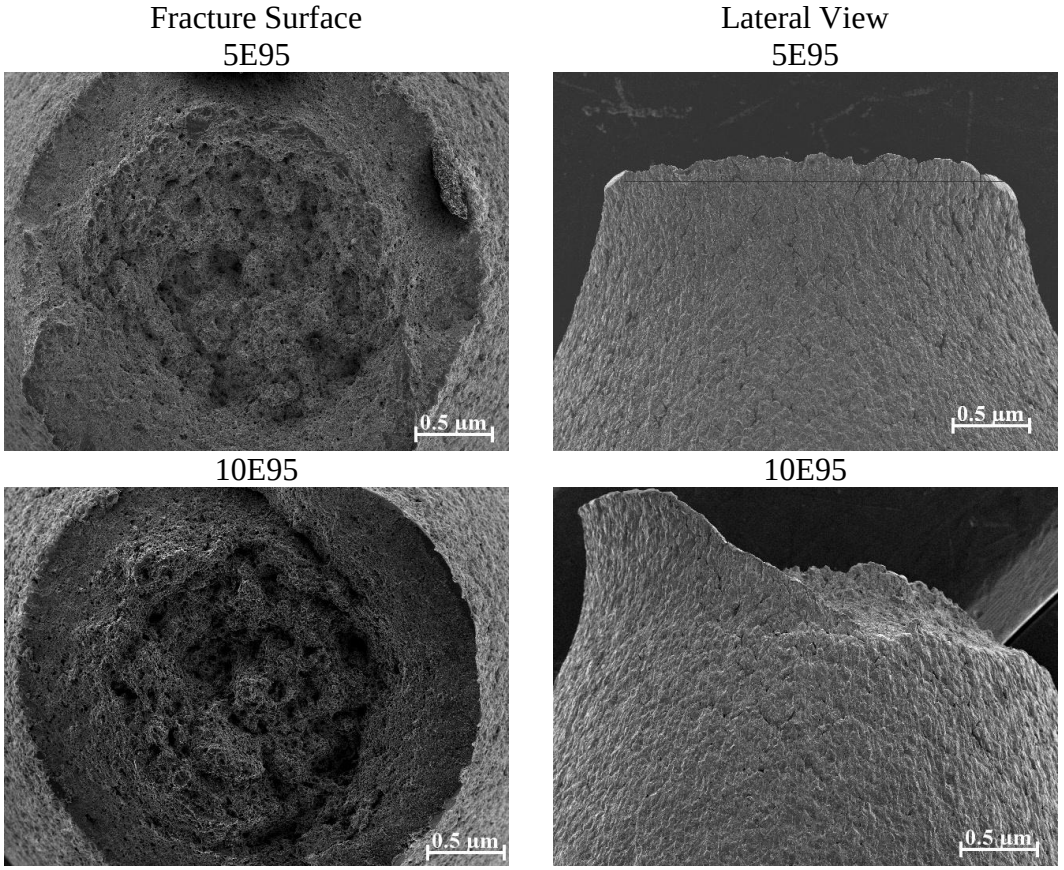

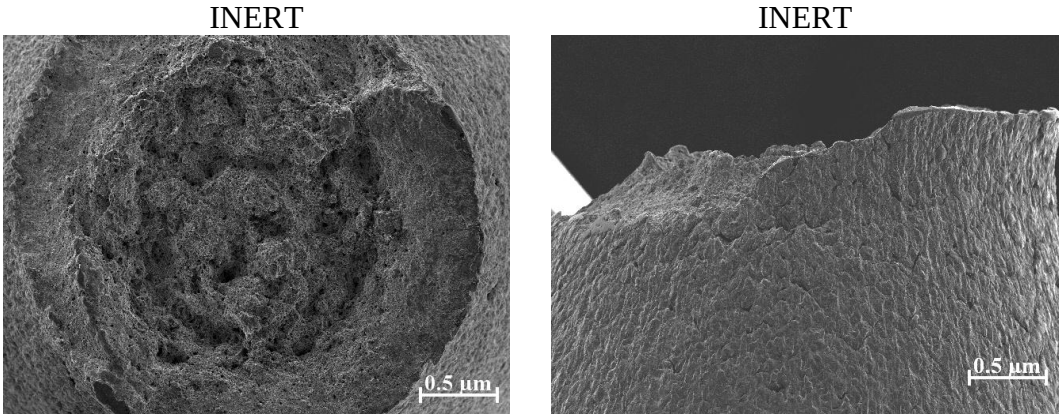

Figure 3. SEM images of a) fracture surface showing ductile failure and b) lateral view with no sign of SCC cracks, for specimens exposed to solutions with water content of 5 V%, 10 V% and inert media.

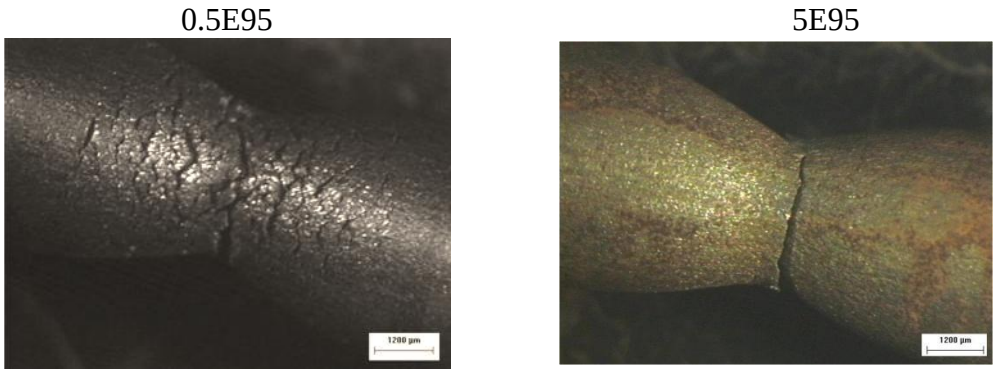

a) **b)**

Figure 4. Optical views of SSRT specimens exposed to a) solution 0.5E95 (secondary crack formation and bright surface) and b) solution 5E95 (oxidized surface without secondary crack formation).

At higher water content, the specimens show a trend towards uniform and localized corrosion, and the potential values approaches the value recorded for the inert media i.e. ≈ 530 mV.

Second, SEM micrographs on fracture surface and lateral views on failed specimens exposed to solutions with water content of 0.5 V%, 1 V% and 2 V%, showed a ductile appearance. However, lateral views for these specimens near the necked region showed extensive secondary cracking, which may indicate some susceptibility to SCC [19], Fig. 2. On the other hand, secondary cracking was not observed for specimens with water content higher than 2 V%, Fig. 3. It is important to point out that the ASTM D 4806 standard calls for a water content of 1 V% maximum. However, the report API D-939 [22] recommends more work on this matter. Since the results of the present work indicates that a water content as low as 0.5 V% may induce a mildly susceptibility to SCC, care should be taken regarding water content values in ethanol blend issues, in particular for small concentrations. Thus, water content higher than 2 V%, does not promotes SCC. Instead, a tendency for general corrosion (and possibly pitting) is observed, see Fig. 4, with this being in agreement with the work of Lou et al.

[23]. From the above, it appears that solutions of E95 blend with water content from 0.5 V% up to 2 V% might cause a mildly SCC susceptibility.

3.2 Electrochemical Noise

ECN measurements were carried out simultaneously with the SSRT tests. For all of them, the statistical analysis of potential and current time series was done at the point of maximum stress.

Figure 5 shows the potential-time series for the specimens exposed in solution 0.5E95 where it can be seen that the anodic peaks are of slightly more amplitude than the ones observed for solutions with higher water content. This fact may correspond with an anodic dissolution process, and also of many other processes occurring simultaneously, for instance, the continuous exposure of fresh surface areas as consequence of secondary cracking. The current-time series show anodic and cathodic transients of high amplitude and low frequency, which could be associated with a localized corrosion process which confirms the behavior observed in the potential-time series [24].

For the X-52 steel exposed in solution 1E95, the anodic and cathodic transients are smaller compared to the ones recorded for solution 0.5E95**,** Fig. 6. However, the tendency observed show anodic transients of larger amplitude, which very likely indicates a continuous rupture and repassivation process.

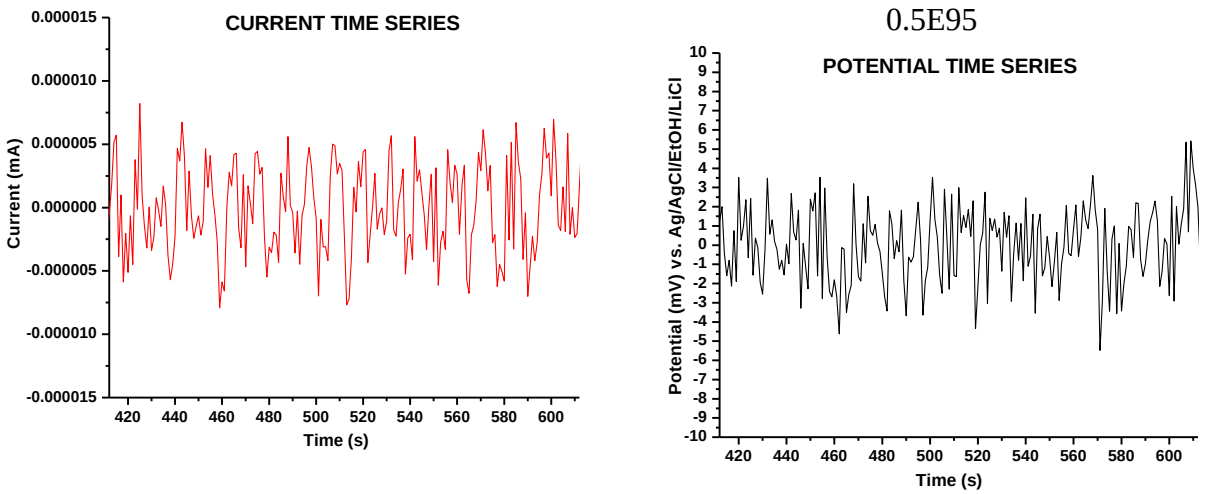

Figure 5. (a) Current and (b) Potential time series recorded at the maximum stress point for X-52 steel in E95 blend with 0.5 V% water content at room temperature.

The current-time series show anodic and cathodic transients of average amplitude of $\pm 6 \times 10^{-6}$ A. These transients are of small amplitude as compared to the ones recorded for solution 0.5E95. Here, noise records depend upon crack formation as a function of rupture and repassivation events.

Potential-time series for samples exposed in solution 5E95 shows an increase in its anodic and cathodic transients frequency, Fig 7. Nevertheless, these transients show a tendency of uniform fluctuations, which could be associated with a general (uniform) corrosion process. Since the current-

time series here show uniform fluctuations of anodic and cathodic transients, this fact corroborates the previous statement.

Figure 8 shows the potential-time series recorded for solution 20E95. The transients frequency is higher in comparison with samples exposed in solution 5E95 but of smaller amplitude, with uniform cathodic and anodic transients, somehow indicating a general corrosion process.

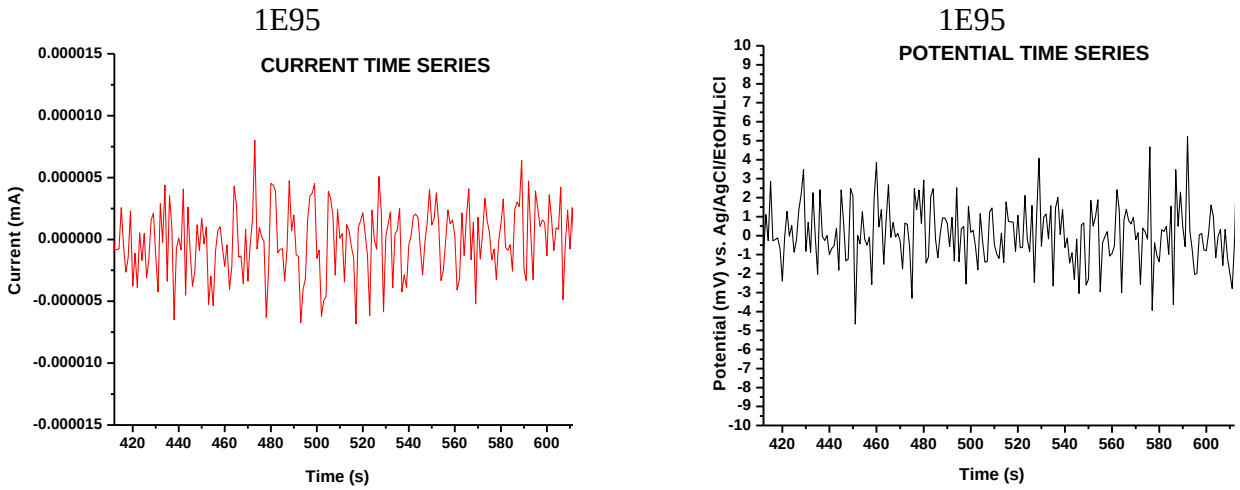

Figure 6. (a) Current and (b) Potential time series recorded at the maximum stress point for X-52 steel in E95 blend with 1 V% water content at room temperature.

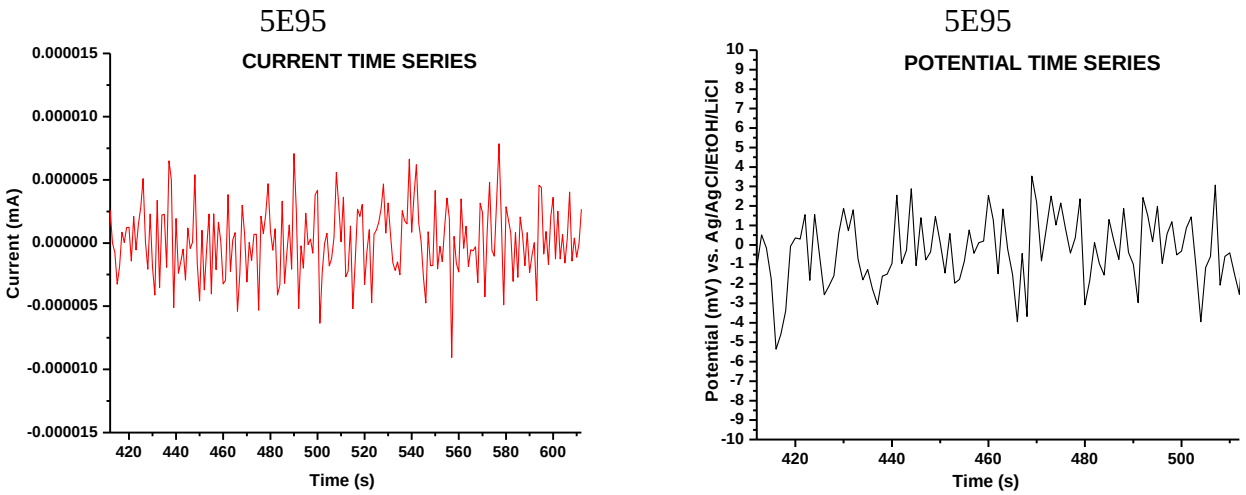

Figure 7. (a) Current and (b) Potential time series recorded at the maximum stress point for X-52 steel in E95 blend with 5 V% water content at room temperature.

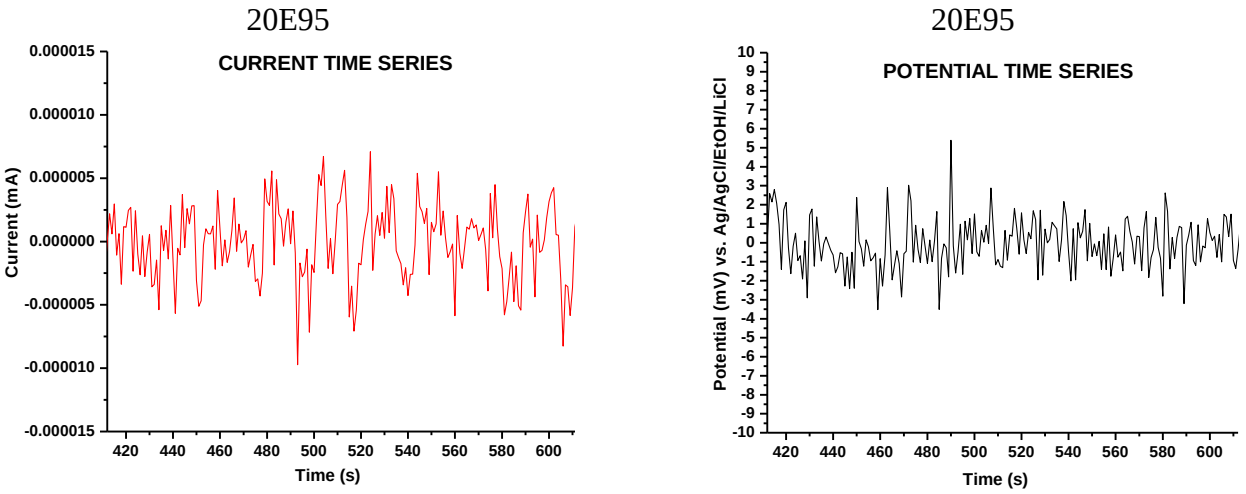

Figure 8. (a) Current and (b) Potential time series recorded at the maximum stress point for X-52 steel in E95 blend with 20 V% water content at room temperature.

The current-time series shows good anodic and cathodic transients stability. This could be due to the fact that for each small variation of anodic potential, there is an immediate cathodic response and vice versa [25-26].

To corroborate the above statement, windowing of potential-time series was carried out. Here, 24 points on the maximum stress zone were taken for analysis. For the sake of comparison, only the samples exposed to solutions 0.5E95 and 20E95 were considered.

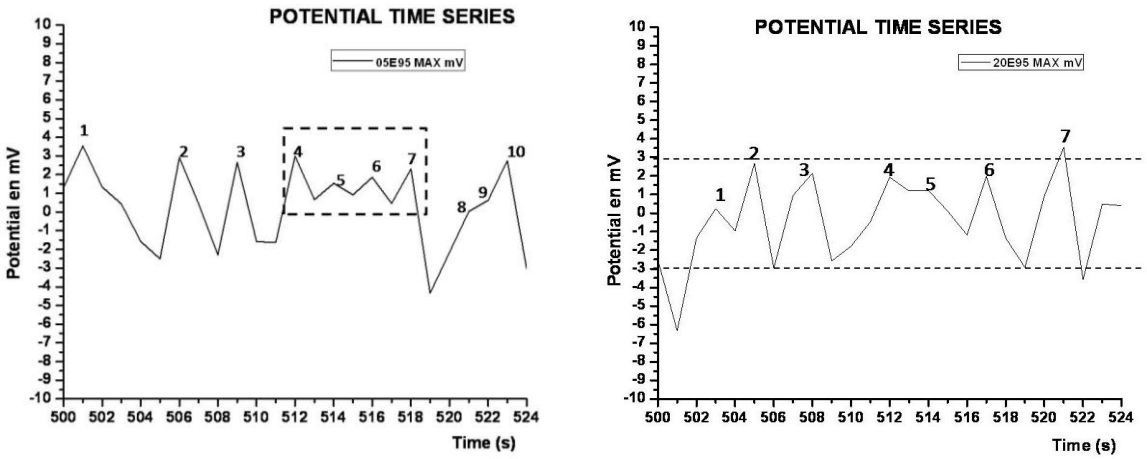

(a) (b)

Figure 9. Windowing of potential-time series corresponding to the electrochemical response in solution 0.5E95 (Fig. 5b) and in solution 20E95 (Fig. 8b).

In the first case (lower water content), a general trend for the transients to be located mainly at the cathodic side was observed, see peaks 4,5,6,7 in Fig. 9 (a) This probably indicates that the material is forming a passive film. However, if the transients remain mainly at the anodic side, this could be indicative of a localized corrosion process. In the second case (20E95), potential fluctuations of low

amplitude become more stable i.e. in general similar anodic and cathodic fluctuations occurred, Fig. 9 (b). This behavior, which can be associated with a general corrosion process, was observed mainly in solutions with water content above 2 V% [27].

The analysis of ECN signals in experiments coupled with SSRT test involves constant exposition of new surfaces which can be susceptible of damage for a given environment. Thus, the response obtained will depend upon the material tested, strain rate and corrosive media.

3.3 Linear Polarization Resistance (LPR)

Table 5 shows the values of polarization resistance (Rp), corrosion potential (E_{corr}) and I_{corr} obtained. Significant differences can be noted among the various solutions used. For solutions containing less than 2 V% water, very high Rp values were recorded, whereas for higher water content, the Rp values recorded changed significantly. The values of E_{corr} for the solutions with the lower water content lie around -100 to 0 (mV vs Ag/AgCl/EtOH/LiCl) whereas for higher water content E_{corr} values around -200 mV vs Ag/AgCl/EtOH/LiCl were recorded.

Table 5. Rp, Icorr and Ecorr measured for the various solutions used.

Solution	Rp (Ohm.cm²)	Icorr (mA/cm²)	Ecorr (mV vs. Ref. Electrode)
0.5E95	1.75E+05	2.26E-04	-321.62
1E95	1.97E+05	2.04E-04	-112.49
2E95	6.88E+04	5.75E-04	-14.28
5E95	4.89E+04	8.09E-04	-115.43
10E95	1.25E+04	3.16E-03	-131.71
20E95	6.04E+03	6.55E-03	-154.86

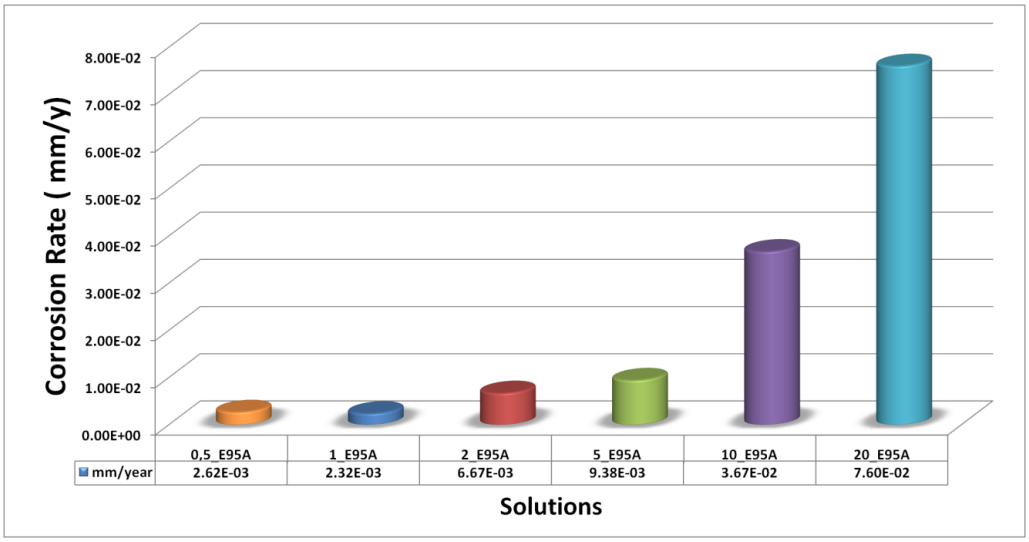

Figure 10. Corrosion rates determined by LPR for the X-52 steel exposed in E95 blend with various water concentrations (V%) at room temperature.

Figure 10 shows the corrosion rates derived from the LPR method. A difference of about one order of magnitude can be noted between specimens exposed to solutions with low (less than 2 V%) and higher (5 V%, 10 V% and 20 V%) water content.

3.4 Weight Loss Measurements.

Samples were immersed into the various E95 blend solutions for 30, 60 and 90 days. As an example, Fig. 11 show a general view for X-52 specimens exposed 60 days into 05E95 and 20E95 solutions. The samples exposed to the E95 blend with the lower water content (0.5 V%) showed much less corrosion products formation as compared with the higher water content solution (20 V%).

In the former case, small water content may cause only a localized corrosion process; in the latter case, water content above 2 V% may induce a general corrosion process. SEM surface observations confirm the previous statements, Fig. 12.

Figure 11. General view of X-52 specimens after exposure for 60 days into a) 05E95 solution and b) 20E95 solution.

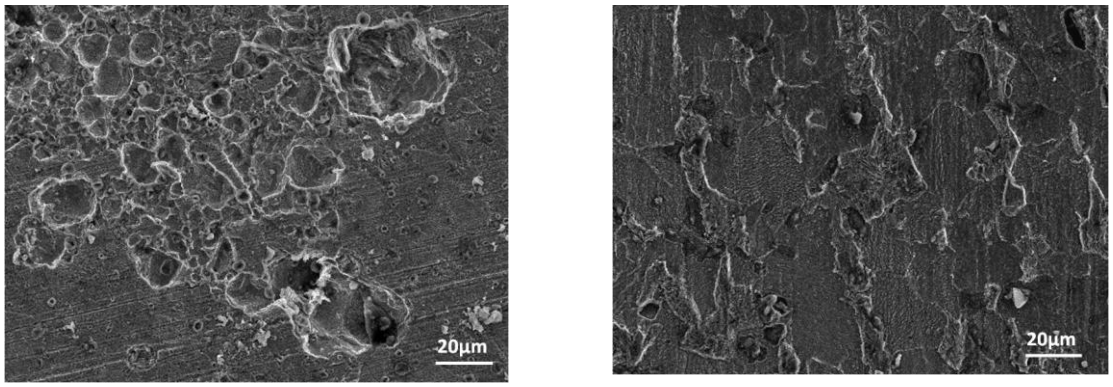

(a) (b)

Figure 12. SEM micrographs of X-52 steel specimens exposed for 60 days in a) 0.5E95 solution exhibiting localized corrosion, and (b) 20E95 solution showing a uniform corrosion process.

Figure 13.shows the weight loss results after 30, 60 and 90 days of exposure to the various solutions. In general, the weight loss data recorded for each solution increases with time. After 90 days, samples exposed in solution 20E95 showed the highest weight loss recorded, whereas the data measured for samples immersed in solution 1E95 showed the lower weight losses.

3.5 pH_e Measurements.

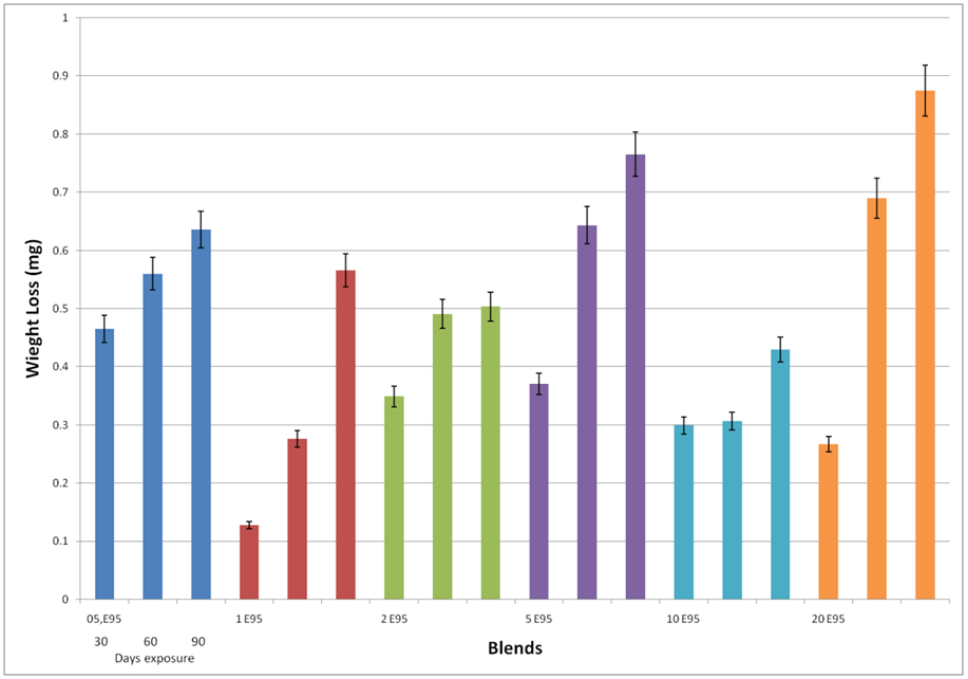

Figure 13. Weight Loss recorded for X-52 steel after 30, 60 and 90 days exposure to the various E95 blend solutions used.

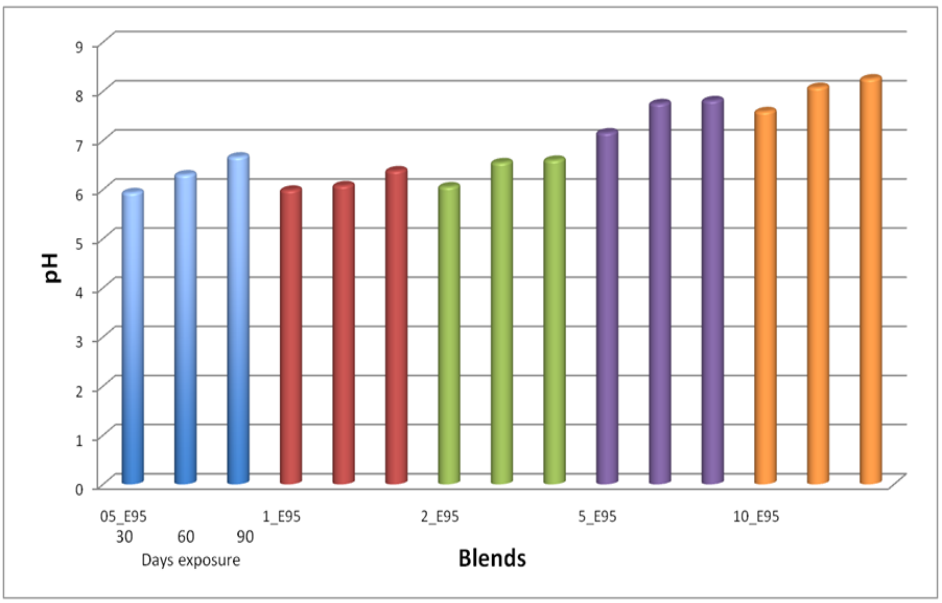

Figure 14. pH_e measured after 30, 60 and 90 days exposure time to the various E95 blend solutions used.

pH_e measurements were taken after 30, 60 and 90 days of exposure to the various solutions, Fig. 14. It can be seen that pH_e values increases with exposure time. Thus, the various solutions tend to be more alkaline with time. To some extent, this fact may indicate a tendency towards the formation of a protective film, which would be easier to form at higher water content [11]. The pH_e value for solution 05E95 used in the SSRT test is very similar to the value measured after 30 days ($pH_e \approx 5.8$) whereas for solution 10E95, a $pH_e \approx 7.8$ was recorded. Fig. 2 shows a failed X-52 steel sample exposed to solution 0.5E95 which showed mildly SCC susceptibility, whereas in the higher pH_e solution 10E95 (Fig. 3) there was no indication of secondary cracking along the necked area of tensile samples. Thus, pH_e values seem to be an important parameter to assess the SCC susceptibility of X-52 steel in fuel-grade ethanol blends.

4. CONCLUSIONS

Based on the results of the present work, the following conclusions can be made:

- For the various solutions used, SCC of X-52 carbon steel depends on the water content**:** samples tested in E95 blend with water content up to 2 V% showed a mildly SCC susceptibility whereas samples tested in higher water concentrations are immune to SCC.
- In general, the maximum stress did not change significantly with water content in the base E95 blend. However, the main difference was observed for the % elongation values.
- SEM observations on fracture surfaces indicate a ductile behavior. However, secondary cracks along the gage length for specimens exposed to water content from 0.5 V% up to 2 V% was observed. To some extent, this indicate a mildly susceptibility to SCC. Higher water content in the ethanolic solution did not produce secondary cracking.
- ECN measurements and analysis indicated that, for low water content solutions, potential and current-time series showed anodic and cathodic transients of high amplitude and low frequency, which could be associated with a localized corrosion process. Higher water content in the E95 blend in general results in similar anodic and cathodic fluctuations which can be associated with a general corrosion process.
- The potential values recorded at maximum stress for samples exposed to solutions with water content of 0.5 V%, 1 V% 2 V%, were -43, -54 and -105.9 (mV vs Ag/AgCl/EtOH/LiCl) respectively. These values might indicate a mildly susceptibility to SCC.
- The LPR results indicated that specimens exposed to solutions with water content up to 2%V exhibited the lower corrosion rates. Above 5 V% water, corrosion rates increases significantly.
- Weight loss decreases for solutions containing less than 5 V% water, but localized corrosion susceptibility increases. Above 2 V% water, weight loss increases and a uniform corrosion process seems to be more likely thus reducing pitting susceptibility. With higher water content in E95 blend, more oxidation products were observed on the specimens surface.
- The pH_e values for solutions containing water content above 2 V% was higher than the ones measured for lower water concentrations. In the former case, there was no indication of SCC, whereas in the latter a mildly SCC susceptibility was noted. Thus, alkaline conditions seem to

decrease the SCC susceptibility of X-52 carbon steel. In addition, pH_e measurements indicate a tendency to higher values as a function of time.

ACKNOWLEDGEMENTS
The authors wish to thank the financial support (project 106042) from Consejo Nacional de Ciencia y Tecnología (CONACYT) Mexico. Also, technical assistance from K. Campos-Venegas, W. Antunez-Flores, L. de la Torre-Saenz, R. Camarillo-Cisneros, G. Vázquez-Olvera and J. Y. Achem-Calahorra is appreciated.

References

1. K. Reid, (2007) http://www.npnweb.comsid=901D2CC3506F4C1187DF5BE4A8A2C0FF&nm=News&type=MultiPublishing&mod=PublishingTitles&mid=8F3A7027421841978F18BE895F87F791&tier=4&id=78CD75DC8ACF4556A537086D8388D3C2.
2. F. Hernández-Sobrino, C. Rodríguez-Monroy, J. L. Hernández-Pérez, *Renew.Sust. Energ. Rev.*, 14 (2010) 3076.
3. C. Berlanga-Labari, A. Albistur-Goñi, I. Barado-Pardo, M. Gutierrez-Peinado, J. Fernández-Carrasquilla, *Mater. Design*, 32 (2011) 441.
4. U.S. Department of Energy, Biomass program, *Washington Energy Efficiency and Renewable Energy (EERE)*, (2012), http://www1.eere.energy.gov/biomass/ethanol_ myths_facts.html.
5. A. Albistur-Goñi, C. Berlanga-Labari, J. Fernández-Carrasquilla, Anales de Mecánica de la Fractura, 1 (2008) 193.
6. J. Beavers, F. Gui, N. Sridhar, NACE International, Corrosion 2010, San Antonio, TX., (2010) paper 10072.
7. G. K. Pedraza-Basulto, MSc. Thesis, Centro de Investigación en Materiales Avanzados S.C. Chihuahua, Chih., Mexico. (2009).
8. ASTM D 4806, "*Standard Specification for Denatured Fuel Ethanol for Blending with Gasolines for Use as Automotive Spark-Ignition Engine Fuel*" ASTM International, West Conshohocken, PA. (2007).
9. N. Sridhar, K. Price, J. Buckingham, J. Dante, *Corrosion* 62 (2006) 687.
10. G. Copabianco, G. Farina, G. Faita, C.A. Farina, *International Congress on Metallic Corrosion*, Toronto, Canada: National Research Council of Canada, 3 (1984) 532.
11. X. Lou, D. Yang, P. M. Singh, *Corrosion Sci.*, 65 (2009) 785.
12. R.D. Kane, N. Sridhar, M.P. Brongers, J.A. Beavers, A. K. Agrawal, L.J. Klein, *Mater. Performance* 44 (2005) 50.
13. ASTM G129, *"Standard Practice for Slow Strain Rate Testing to Evaluate the Susceptibility of Metallic Materials To Environmentally Assisted Cracking"* ASTM International, West Conshohocken, PA. (1995).
14. NACE TM011-11, "*Slow Strain Rate Test Method for Evaluation of Ethanol Stress Corrrosion Cracking in Carbon Steels*", (2011).
15. Y. Tan, *Corrosion Sci.*, 53 (2011) 1145.
16. M. Stern, A. L. Geary., *J. Electrochem. Soc.*, 104 (1957) 56.
17. ASTM G1,*"Standard Practice for Preparing, Cleaning, and Evaluating Corrosion Test Specimens"* ASTM International, West Conshohocken, PA. (2003).
18. ASTMD 6423, "*Determination of pH_e of Ethanol, Denatured Fuel Ethanol, and Fuel Ethanol"* ASTM International, West Conshohocken, PA. (1999).
19. D. R. McIntyre, R. D. Kane, S. M. Wilhelm, *Corrosion*, 44 (1988) 920.

20. F. Gui, N. Sridhar, J. Beavers, *NACE International Corrosion 2009*, Atlanta Georgia.(2009) paper 09531.
21. J. G. Maldonado, N. Shidhar, *NACE International 2007*, Houston, TX., (2007) paper No. 07574.
22. R. Kane, D. Eden, S. Srinivasan, J. Maldonado, A. Agarwal, J. Beavers, API Technical Report 939-D, *API, Publishing Services*, Washington, D. C. (2007).
23. X. Lou, L. R. Goodman, P. M. Singh, D. Yang, *NACE International 2010*, San Antonio TX., (2010) paper 10073.
24. J. M. Malo-Tamayo, J. Chavarín-Uruchurtu, *Técnicas Electroquímicas para el Control y Estudio de la Corrosión, Capitulo 4, UNAM*, México D.F., ISBN: UNAM 970-32-0540-2. (2003) 93.
25. F. J. Botana-Pedemonte, A. Aballe-Villero, M. Marcos-Barcena, Ruido Electroquímico Métodos de Análisis, *Septem Ediciones*, Asturias España ISBN: 84-95687-33-X. (2002) 128.
26. G. K. Pedraza-Basulto, A.M. Arizmendi-Morquecho, A. Borunda-Terrazas, R. Bautista Margulis, A. Martínez-Villafañe, J.G. Chacón-Nava, XXI International Materials Research Congress, Cancún, México, ISBN: 978-607-95042-8-1, (2012) paper 39.
27. J. R. Kearns, "*Electrochemical Noise Measurement for Corrosion Applications"* ASTM Publications (PCN) 04-012770-27, ISBN: 0-8031-2032-X (1996).